Research Article

Journal of Environmental Nanotechnology

Synthesis and Characterization of Pure and Copper-doped Zinc Oxide Nanoparticles

A. Saranya*, N. Vidhya, V. Kalaiselvi, K. Surya, V. Ramya
Department of Physics, Navarasam Arts and Science College for Women, Erode, TN, India
Received: 26.01.2020 Accepted: 07.03.2020 Published: 30-06-2020
*saranyaarjunan711@gmail.com

ABSTRACT

In this work, the zinc oxide (ZnO) nanoparticles were successfully synthesized using both biological and chemical techniques. Pure and Cu-doped Zinc oxide nanoparticles were prepared by co-precipitation method associated with microwave irradiation method; they were characterized by XRD, SEM, EDAX and UV techniques. The X-ray diffraction pattern analysis revealed the crystalline size of the nanoparticles. The morphology and purity of the sample were analyzed by Scanning electron microscopy and Energy Dispersion X-ray Diffraction analysis. The optical properties were ascertained by Ultraviolet spectroscopy. The results matched well with the standard values.

Keywords: Pure zinc oxide; Copper-doped zinc oxide; Crystalline size; Morphology; Optical properties.

1. INTRODUCTION

Nanotechnology mainly focuses on the synthesis of nanoparticles of various sizes, shapes and compositions involved in several applications. Nanomaterials are believed to be next-generation molecules with huge potential in diverse fields, including medicine, catalysis and sensors. Zinc oxide (ZnO) is considered as one of the most important oxide materials due to its unique features and wide range of technologically important applications (Kalaiselvi *et al.* 2014; 2018).

ZnO is an n-type semiconductor; moreover, it is cheap and environment-friendly as compared to other metal oxides. Due to these qualities, it has found potential applications in fields such as gas sensors, solar cells, varistors, light-emitting devices, photocatalysts, antibacterial activity and cancer treatment (Shreema *et al.* 2020; Kaphle *et al.* 2019). ZnO lacks a centre of symmetry, making it beneficial for its use in actuators and piezo-electric transducers. Several methods have been devoted to the fabrication of transition metal-doped ZnO nanoparticles (Bhuyian and Rahman, 2014). Among these methods, the co-precipitation method is of great interest because of its simplicity, low equipment cost, relatively lower processing temperature and environmentally benign nature (Wu *et al.* 2014). This method is advantageous over other methods because the reagents are mixed at the molecular level, and therefore, there is good control of stoichiometry, morphology, purity and homogeneity (Tan *et al.* 2014; Subramaniyan *et al.* 2019).

Properties of ZnO can be tuned according to the research interest by doping with various metal atoms to suit specific needs and applications (Uhm *et al.* 2013). Metal doping induces drastic changes in the optical, electrical and magnetic properties of ZnO by altering its electronic structure. Many authors have reported the changes induced by the incorporation of transition metal ions into ZnO lattice (Alkahlout *et al.* 2014; Ansari *et al.* 2015; Khan *et al.* 2016). Albeit a large number of reports on transition metal-doped ZnO system, very less work is done on Cu-doped ZnO. Substitution of copper into the ZnO lattice (Krstulovic *et al.* 2018) has improved properties such as photocatalytic activity, gas sensitivity and magnetic semi-conductivity (Fang *et al.* 2018; Mahapatra *et al.* 2016). Copper-doped zinc oxide was found to exhibit ferromagnetic performance at room temperature. Photoluminescence (PL) of Cu-doped ZnO nanocrystals were found to show pronounced UV emission and negligible visible emission with peak positions coinciding with that of undoped ZnO. Literature shows the substitution limit of Cu in ZnO to be low (around 5%). An attempt has been made in this work to synthesize a higher compositional level of copper-doped ZnO lattice. The present investigation deals with the synthesis of Cu-doped ZnO nano-powders with copper content varying from 5 to 30% via co-precipitation method, followed by the characterization of samples using Transmission Electron Microscopy (TEM), Powder X-ray Diffraction (XRD) and Fourier Transform Infrared Spectroscopy (FT-IR) techniques. The influence of Cu content on the structural and electrical properties has been investigated (Singhal *et al.* 2012).

2. MATERIALS & METHODS

Zinc acetate dihydrate ($C_4H_{10}O_6Zn$) is a moderately water-soluble crystalline zinc source that decomposes to zinc oxide on heating. Copper sulphate is an inorganic compound that combines sulphur with copper. 4.9 g of Zinc acetate dihydrate were taken in a beaker with 50 ml of distilled water. The solution was stirred for 30 minutes. Moreover, 0.6242 g of $CuSO_4$ was taken in another beaker with 50 ml of distilled water. This solution was stirred for 30 minutes. The $CuSO_4$ solution was added into zinc acetate dihydrate solution. Both solutions were stirred for 30 minutes. Then 5 g of $Na(OH)_2$ was taken and dissolved in 10 ml of distilled water. This NaOH solution was added drop-by-drop into Cu-doped ZnO solution, till the pH reached up to 12 and then stirred for 45 minutes. The prepared solution was aged for one day at room temperature and then the precipitates were washed with distilled water and dried for 35 minutes in a domestic microwave oven at 70 W. Finally, the nanopowder was ground by using mortar**.**

For pure ZnO powder preparation, 10.975 g of zinc acetate dihydrate was taken in a beaker with 150 ml of distilled water. The solution was stirred for 30 minutes. Then 5 g of $Na(OH)_2$ was taken and dissolved in 10 ml of distilled water. The Na(OH) solution was added drop-by-drop into the zinc acetate dihydrate solution, until pH reached 12 and then stirred for 30 minutes. The prepared solution was aged for one day at room temperature and then the precipitates were washed with distilled water and dried for 45 minutes in a microwave oven at 70 W. Finally, the nanopowder was ground by using mortar**.**

3. CHARACTERIZATION TECHNIQUES

3.1 FTIR

FTIR is an analytical technique used to identify the functional groups of prepared samples. The spectrum was recorded in the range of 4000-400 cm^{-1} region (Ghorbani *et al.* 2015).

3.2 XRD

In XRD, interaction of a particular crystalline solid with X-rays helps in investigating its actual structure. Crystals are found to act as diffraction gratings for X-rays, and this indicates that the constituent particles in the crystals are arranged in planes at close distances in repeating patterns.

The lattice parameters were calculated by the equation,

$$1/d^2 = (4(h^2+hk+k^2)/3a^2) + (l2/c^2)$$

The crystalline size of the particle was defined by Debye-Scherrer's formula,

$$D = k\lambda/\beta \cos\theta$$

where, D is the average crystalline size, k is the broadening constant, λ is the wavelength, β is the full width half-maximum and θ is the Bragg's angle.

3.3 EDAX AND SEM

Energy dispersive spectroscopy is used to identify the elemental composition of the sample. The surface morphologies of synthesized ZnO samples were analysed using Scanning Electron Microscopic analysis (SEM).

3.4 UV AND PL

UV-Vis. and Photoluminescence spectroscopies identified the optical properties of the samples.

4. RESULTS

4.1 FTIR Analysis

The Fourier transform infrared spectra of pure and Cu-doped ZnO nanoparticles are shown in Fig. 4.1. FTIR is used to investigate the functional elements in the synthesized nanoparticles. FTIR identifies chemical bonds in a molecule by producing an infrared absorption spectrum. The FTIR spectrum of the prepared pure and capped ZnO samples were plotted between the wavelength ranges from 4000 to 500 cm^{-1}. Absorption peaks at 3733.72 cm^{-1} and 3882.70 cm^{-1} corresponded to the O=H stretching band. The peaks at 2298.72 cm^{-1} and 2353.15 cm^{-1} indicated the C=H bond. The absorbance at 2800 cm^{-1} and 2793.15 cm^{-1} represented the C=H bond. The absorption peaks at 1689.26 cm^{-1} and 1724.36 cm^{-1} indicated the presence of H=O=H stretching. And then, C=HO stretching absorption was represented by the peaks at 1153.69 cm^{-1} and 1170.79 cm^{-1}, respectively. The results indicate that the synthesized ZnO nanoparticles were stabilized by the chemical molecular constituents present in the copper-doped particles (Table 1).

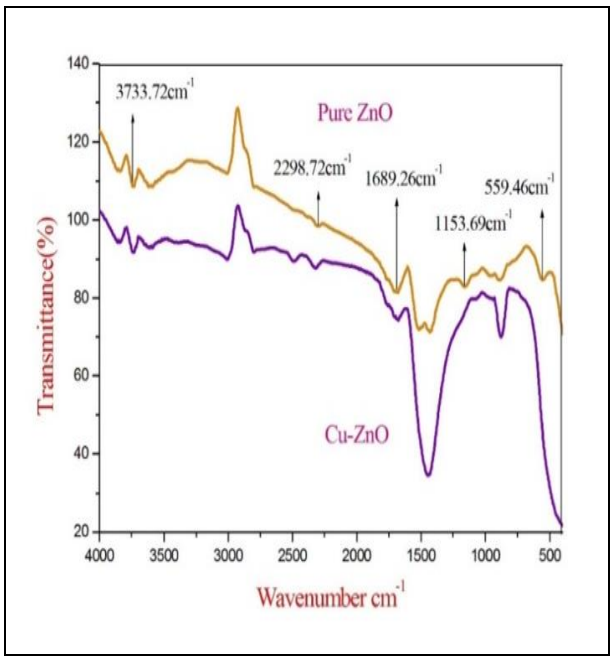

Fig. 1: FTIR spectrum of Pure and Cu-doped ZnO nanoparticles.

4.2 EDAX

The chemical composition of the elements was determined by Energy-dispersive X-ray spectroscopy. The EDAX analysis of pure and Cu-doped ZnO were shown in Fig. 2 (a) and (b). The functional groups of Cu, Zn and O were present in the sample. It confirmed the purity of the composition elements (Table 2).

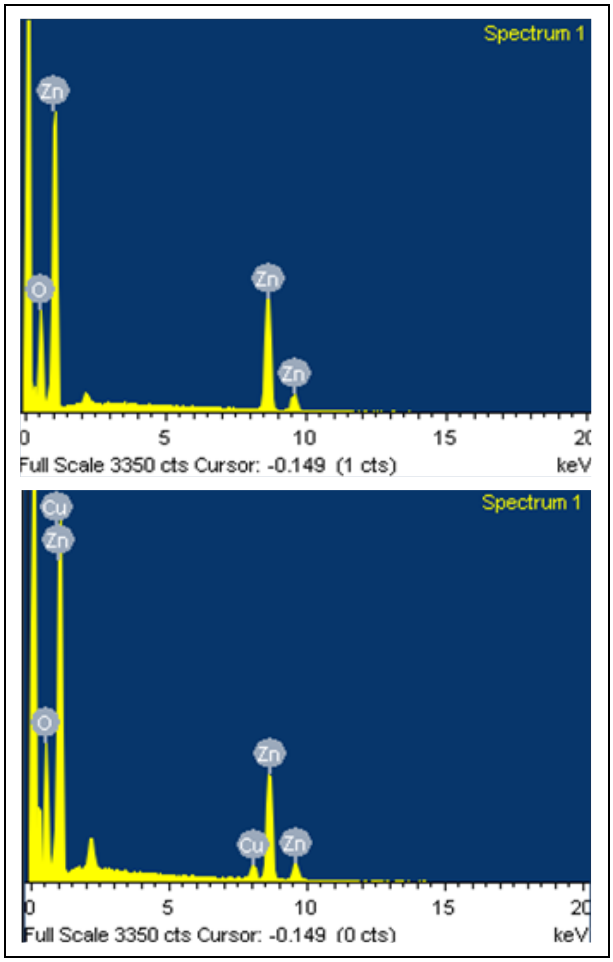

Fig. 2: EDAX spectrum of Pure and Cu-doped ZnO NPs .

Table 1. FTIR functional group of pure and Cu-doped ZnO nanoparticles.

S. No.	Sample Name	Wave Number (cm^{-1})				
		O=H Stretching vibration	C=H Stretching vibration	H=O=H Stretching vibration	C=HO Stretching vibration	Zn=O Stretching vibration
1	Pure ZnO	3733.72	2298.72	1689.26	1153.69	559.46
2	Cu-doped ZnO	3882.70	2353.15	1724.36	1170.79	557.42

Table 2. EDAX spectrum of pure and Cu-doped ZnO nanoparticles.

Sample	Element	Approx. Conc.	Intensity Corrn.	Weight %	Weight % Sigma	Atomic %
Cu-doped ZnO	O K	28.02	1.1911	31.98	0.66	65.59
	Cu K	4.88	0.9111	7.28	0.47	3.77
	Zn K	40.72	0.9114	60.74	0.72	30.54
Pure ZnO	O K	21.88	1.1241	26.42	0.69	59.46
	Zn K	50.17	0.9258	73.58	0.69	40.54

4.3 XRD

The XRD pattern of prepared Pure ZnO and Cu-doped ZnO were shown in Fig. 3. The prepared sample confirmed the presence of a hexagonal structure. The diffraction peaks of the prepared pure ZnO at 2θ =36.44, 63.03, 68.1 and 69.29 and then the diffraction peaks of Cu-doped ZnO at 2θ=36.29, 62.89, 67.98 and 69.07 were identified. Both were corresponding to the hkl planes (101), (103), (112) and (201). The average crystalline size (D) of pure ZnO and Cu-doped ZnO were 18.67 and 16.25 nm, respectively. Thus the average crystalline size of pure ZnO was higher than the Cu-doped ZnO due to the capping of Copper. The unit cell volume (V) and the lattice parameters (a and c) decreased due to an increase in crystalline size (Table 3).

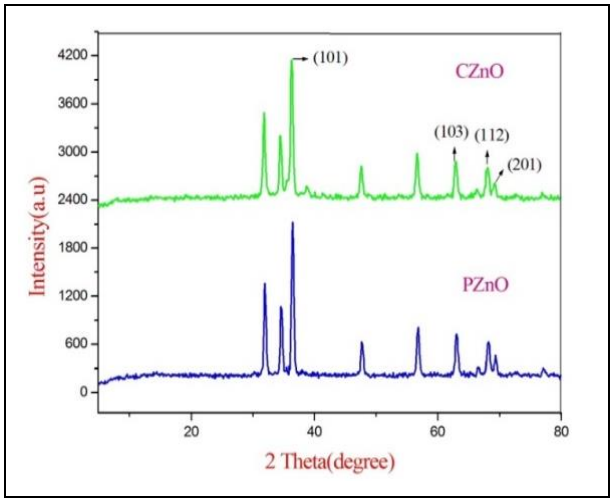

Fig. 3: XRD patterns of pure and Cu-doped ZnO NPs.

4.4 SEM Analysis

The morphological structure of the prepared nanocomposites was revealed in SEM. The synthesized micrographs of pure (Fig. 4 a and b) and Cu-doped ZnO nanoparticles (Fig. 4 c and d) were crystalline; both were having needle-shaped nanostructure. The particle size of the pure ZnO was 25.45 to 103.36 nm in diameter and Cu-doped ZnO was 25.71 to 74.97 nm in diameter.

4.5 UV-Vis Analysis

UV-Vis spectra of pure ZnO and Cu-doped ZnO nanoparticles were shown in Fig. 6. The spectra were recorded in the range of 200 to 750 nm. Samples exhibited the absorbance peaks in the UV region. The presence of maximum absorbance peak was around 356 nm in pure and Cu-doped ZnO samples.

Table 3. SEM spectrum of pure and Cu-doped ZnO nanoparticles.

Sample	2 theta (deg)	FWHM (deg)	D (Å)	Intensity (Counts)	Crystalline size (nm)	Average crystalline size (nm)	hkl	Lattice constants		Unit cell volume (V)
								a=b	c	
Pure ZnO	36.44	0.4703	2.46	1195	17.78	18.67	101	3.22	5.20	47.71
	63.03	0.5020	1.47	358	18.56		103			47.53
	68.12	0.5205	1.37	292	18.42		112			46.41
	69.29	0.4849	1.35	163	19.91		201			46.80
Cu-doped ZnO	36.29	0.5015	2.47	1104	16.67	16.25	101	3.23	5.18	47.18
	62.89	0.5500	1.47	326	16.93		103			46.87
	67.98	0.6090	1.37	267	15.73		112			46.77
	69.07	0.6159	1.35	123	15.66		201			47.04

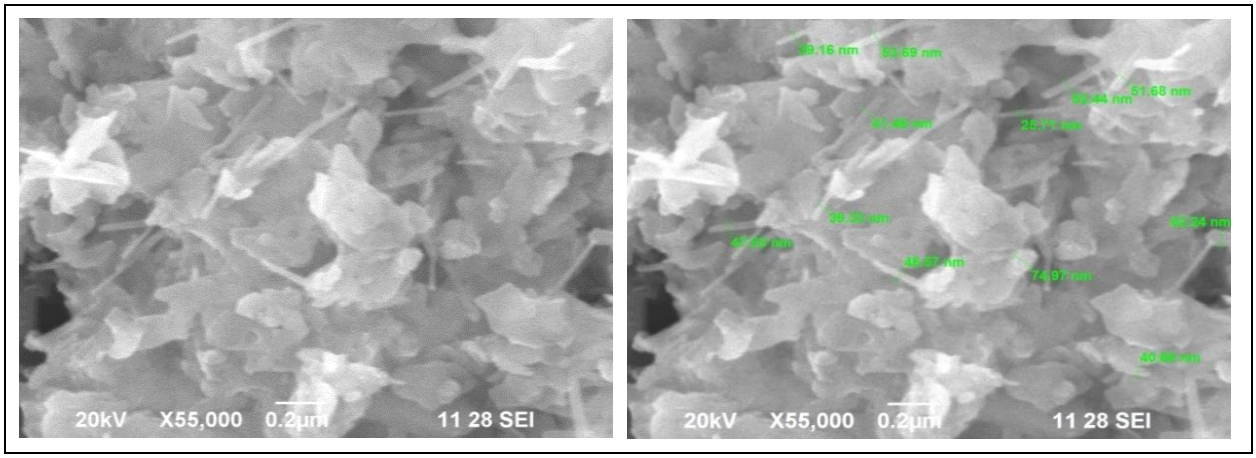

Fig. 4: SEM analysis of pure ZnO nanoparticles.

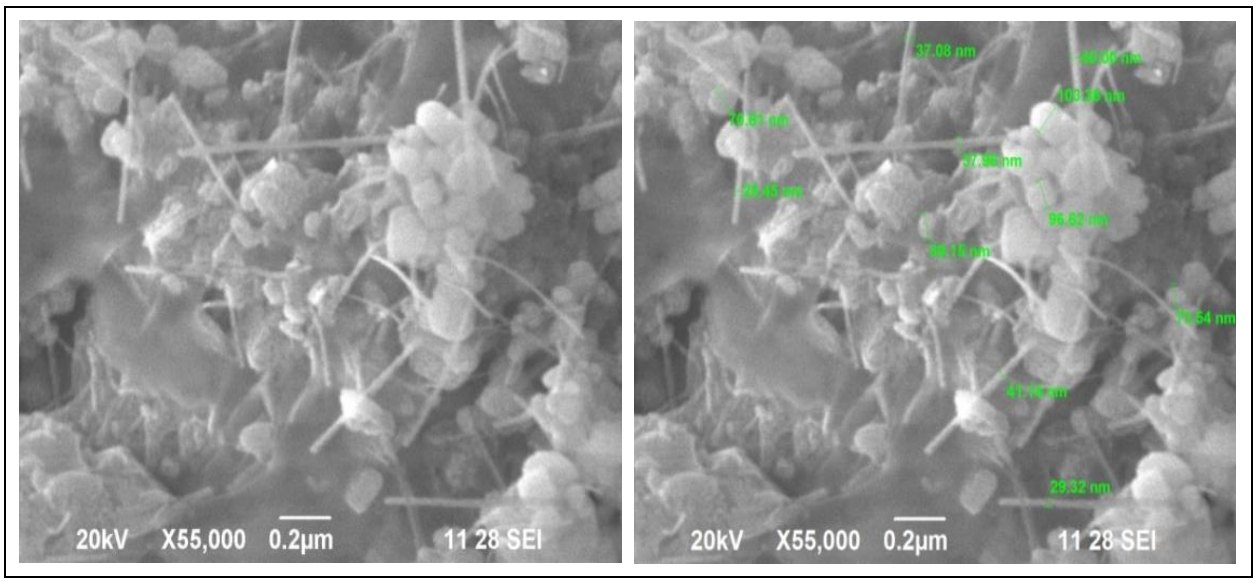

Fig. 5: SEM analysis of pure and Cu-doped ZnO nanoparticles.

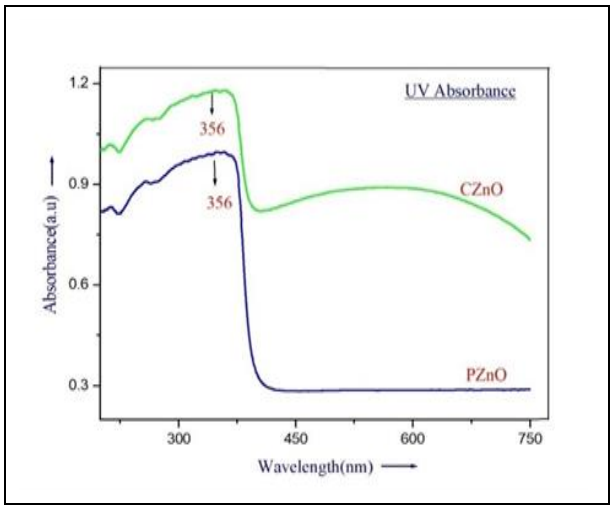

Fig. 6: UV-Vis. spectrum of pure and Cu-doped ZnO NPs.

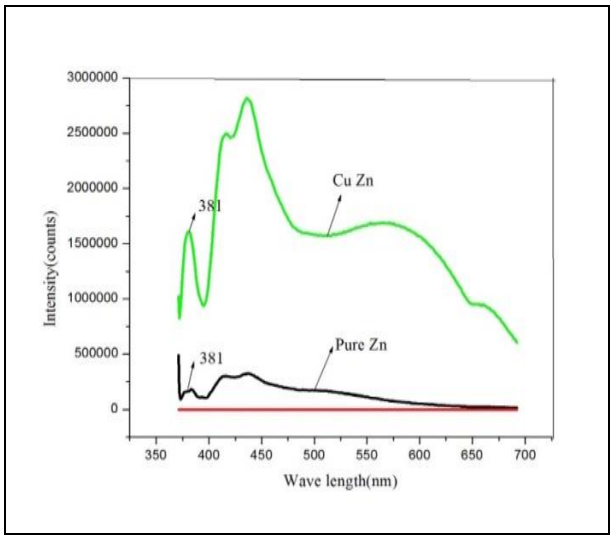

Fig. 7: PL analysis.

Table 4: UV-Vis. spectrum of pure and Cu-doped ZnO NPs.

S. No.	Sample Name	Wave Length nm)	Band Gap Energy (eV)
1.	PZnO	356	3.42
2.	CZnO	356	3.42

4.6 PL Analysis

Fig. 7 depicts the emission radiations of pure and Cu-doped ZnO, based on Photoluminescence spectroscopy analysis. For both pure and Cu-doped ZnO, the excitation wavelength was in 378 nm band. Pure ZnO has a normal bandgap energy of 3.31 eV, while the measured bandgap energy of both samples were 3.42 eV.

5. CONCLUSION

In this work, the zinc oxide nanoparticles were synthesized by using with and without the doping agent of copper sulphate and were characterized by FTIR, EDAX, XRD, SEM, UV and PL.

- The FTIR analysis has shown the different functional groups present in the given samples of pure and Cu-doped ZnO nanoparticles.
- EDX has revealed the chemical elements present in the prepared samples. The pure and Cu-doped zinc oxide nanoparticles were having Zinc (Zn), Oxide (O) and Copper (Cu).

- XRD pattern has confirmed the presence of hexagonal structure, and it is used to determine the crystalline size of the sample and unit cell dimensions of the prepared samples.
- SEM has shown the morphological structure of the prepared samples and revealed the needle shapes for both the samples.
- UV-Vis. spectrum has shown the bandgap energy and wavelength for pure and Cu-doped ZnO NPs - 3.42 eV.
- PL analysis has revealed the bandgap energy and optical absorption characteristics of the samples.

FUNDING

This research received no specific grant from any funding agency in the public, commercial, or not-for-profit sectors.

CONFLICTS OF INTEREST

The authors declare that there is no conflict of interest.

COPYRIGHT

This article is an open access article distributed under the terms and conditions of the Creative Commons Attribution (CC-BY) license (http://creativecommons.org/licenses/by/4.0/).

REFERENCES

Alkahlout, A., Al Dahoudi, N., Grobelsek, I., Jilavi, M. and De Oliveira, P. W., Synthesis and characterization of aluminum doped zinc oxide nanostructures via hydrothermal route, *J. Mater*., 235638 (2014). https://dx.doi.org/10.1155/2014/235638

Ansari M. M., Arshad, M. and Tripathi, P., Study of ZnO and Mg doped ZnO nanoparticles by sol-gel process. In AIP Conference Proceedings, 1665(1), 050123 (2015).

Bhuiyan, M. R. and Rahman, M. K., Synthesis and characterization of Ni doped ZnO nanoparticles, Int. *J. Manuf. Eng.*, 4(1), 10-17 (2014). https://dx.doi.org/10.5815/ijem.2014.01.02

Fang, M., Tang, C. M. and Liu, Z. W., Microwave-assisted hydrothermal synthesis of Cu-Doped ZnO single crystal nanoparticles with modified photoluminescence and confirmed ferromagnetism, *J. Electron. Mater.*, 47(2), 1390-1396 (2018). https://dx.doi.org/10.1007/s11664-017-5928-4

Ghorbani, H. R., Mehr, F. P., Pazoki, H. and Rahmani, B. M., Synthesis of ZnO nanoparticles by precipitation method, *Orient. J. Chem*., 31(2), 1219-1221 (2015). https://dx.doi.org/10.13005/ojc/310281

Kalaiselvi, V. and Mathammal, R., Synthesis and characterization of pure and triethanolamine capped hydroxyapatite nanoparticles and its antimicrobial and cytotoxic activities, *Asian J. Chem.*, 30(8), 1696-1700 (2018). https://dx.doi.org/10.14233/ajchem.2018.21214

Kalaiselvi, V., Jayamani, N. and Revathi, M., Comparative study of pure ZnO and copper doped ZnO nanoparticles synthesised via Co-precipitation Method, *Int. J. Res. Sci*., 1(2), 73-80 (2014). https://dx.doi.org/10.15613/sijrs/2014/v1i2/67542

Kaphle, A., Reed, T., Apblett, A. and Hari, P., Doping efficiency in cobalt - doped ZnO nanostructured materials, *J. Nanomater.*, 7034620 (2019). https://dx.doi.org/10.1155/2019/7034620

Khan, A., Rashid, A., Younas, R. and Chong, R.. A chemical reduction approach to the synthesis of copper nanoparticles, *Int. Nano Lett*., 6(1), 21-26 (2016). https://dx.doi.org/10.1007/s40089-015-0163-6

Krstulovic, N., Salamon, K., Budimlija, O., Kovač, J., Dasović, J., Umek, P. and Capan, I., Parameters optimization for synthesis of Al-doped ZnO nanoparticles by laser ablation in water, *Appl. Surf. Sci.*, 440, 916-925 (2018). https://dx.doi.org/10.1016/j.apsusc.2018.01.295

Mahapatra, P., Kumari, S., Sharma, S., Simran, Gaurav, K., Kumari, N., Parameshwar Kommu, Prabhakar, P. and Bhattacharyya, A. S., Synthesis of Hydroxyapatite and ZnO nanoparticles via different routes and its comparative analysis, *Mater. Sci. Res. India*, 13(1), 07-13 (2016). https://dx.doi.org/10.13005/msri/130102

Shreema, K., Kalaiselvi, V. and Mathammal, R., Green synthesis and characterization of zinc oxide nanoparticles using leaf extract of evolvulus alsinoides, Studies in Indian Place Names., 40(18), 763-778 (2020).

Singhal, S., Kaur, J., Namgyal, T. and Sharma, R., Cu-doped ZnO nanoparticles: Synthesis, structural and electrical properties, *Phys. B: Condens. Matter.*, *407*(8), 1223-1226 (2012). https://dx.doi.org/10.1016/j.physb.2012.01.103

Subramaniyan, S. B., Vijayakumar, S., Megarajan, S., Kamlekar, R. K. and Anbazhagan, V., Remarkable effect of Jacalin in diminishing the protein corona interference in the antibacterial activity of pectin-capped copper sulfide nanoparticles, *ACS Omega*, *4*(9), 14049-14056(2019). https://dx.doi.org/10.1021/acsomega.9b01886

Tan, T. L., Lai, C. W. and Abd Hamid, S. B., Tunable band gap energy of Mn-doped ZnO nanoparticles using the coprecipitation technique, *J. Nanomater.*, 371720 (2014). https://dx.doi.org/doi:10.1155/2014/371720

Uhm, Y. R., Sun Han, B., Rhee, C. K. and Choi, S. J., Photocatalytic characterization of Fe-and Cu-doped ZnO nanorods synthesized by cohydrolysis, *J. Nanomater.*, 958586 (2013). https://dx.doi.org/10.1155/2013/958586

Wu, X., Wei Z., Zhang, L., Wang X., Yang, H. and Jiang, J., Optical and magnetic properties of Fe doped ZnO nanoparticles obtained by hydrothermal synthesis, *J. Nanomater.*, 792102 (2014). https://dx.doi.org/10.1155/2014/792102